Fine scale simulations of the MAP-IOP2a precipitating system: comparison with radar data and sensitivity to the hail category

Jean-Pierre Pinty, Evelyne Richard, Pierre Tabary

FINE SCALE SIMULATIONS OF THE MAP-IOP2A PRECIPITATING SYSTEM: COMPARISON WITH RADAR DATA AND SENSITIVITY TO THE HAIL CATEGORY

Jean-Pierre PINTY[1] Evelyne RICHARD*[1] and Pierre TABARY[2]

[1]Laboratoire d'Aérologie, Toulouse, France
[2]Météo-France, Toulouse, France

1. INTRODUCTION

During Intensive Observing Periods (IOP) of the Mesoscale Alpine Programme (MAP, see Bougeault et al. 2001) a network of three Doppler radars was operated in the Lago Maggiore Target Area (LMTA). In the afternoon and evening of Sept. 17, 1999 (MAP-IOP2a), a major squall line formed on the foothills of the southeastward facing slopes of the Lago Maggiore region and intensified during its propagation to the east as a three-dimensional convective cluster. This intense orogenic system with lots of lightning impacts and precipitation amounts of more than 70 mm in 6 hours, was well observed by the radars. Additional polarimetric data from radar S-POL (NCAR) revealed rich regions of graupel/hail mixture in convective cells where the vertical velocity, $w \geq 4$ ms^{-1} and the radar reflectivity, $Z \geq 45$ dBZ (Tabary et al., 2001).

The simulation of this event has been conducted at high resolution with the French non-hydrostatic model MésoNH (Lafore et al., 1998). An earlier study made by Richard et al. (2002) emphasized the importance of the analysis to conclude that in this case, best results are obtained when the mesoscale model is initialized and forced with ECMWF analyses. MésoNH is run with the grid nesting technique for horizontal grid-sizes of 32, 8 and 2 km. In the innermost domain, cloud and precipitation are entirely resolved by the explicit microphysical scheme. Model outputs are converted in radar reflectivities for comparison with data.

The purpose of this work is to test the impact of heavy rimed particles in the evolution of the MAP-IOP2a precipitating system. In particular, an explicit representation of hail at the 2 km scale is evaluated with a 4-class ice scheme (pristine ice, snow, graupel, hail). The paper is organized as follows. First we briefly describe the microphysical scheme and its extension to incorporate a hail class. Then we present results obtained for different experiments and we conclude on future work.

* *Corresponding author address:*
Evelyne Richard, Laboratoire d'Aérologie, OMP, 14 av. E. Belin, 31650, Toulouse, France;
e-mail <rice@aero.obs-mip.fr>.

2. MICROPHYSICAL SCHEME IN SHORT

2.1 Generalities about the mixed-phase scheme

The scheme is briefly described in Pinty and Jabouille (1998). The full documentation is available from the author or at the web site <http://www.aero.obs-mip.fr/~mesonh/>.

The bulk scheme predicts the evolution of the mixing ratios of six water species: r_v (vapor), r_c and r_r (cloud droplets and rain drops) and r_i, r_s and r_g (pristine ice, snow/aggregates and frozen drops/graupels ordered with an increasing degree of riming). Rain, snow and graupel concentrations are diagnosed as simple power laws $N = C\lambda^x$ where λ is the slope parameter of the size distribution and $C-x$ empirical constants drawn from radar observations. Size distributions follow a generalized γ-law:

$$n(D) = Ng(D) = N\alpha/\Gamma(\nu)\lambda^{\alpha\nu}D^{\alpha\nu-1}exp(-(\lambda D)^\alpha)$$

$g(D)$ is the normalized form. $n(D)$ degenerates into the Marshall-Palmer law for $\alpha = \nu = 1$. As ususally done, simple power laws are taken for the mass-size ($m = aD^b$) and velocity-size ($v = cD^d$) relationships to perform necesary analytical integrations. The complete characterization of each ice category and raindrops is summarized in the table below

Parameters	r_i	r_s	r_g	r_h	r_r
α, ν	3.3	1,1	1,1	1,1	1,1
a	0.82	0.02	196	470	524
b	2.5	1.9	2.8	3.0	3.0
c	800	5.1	124	207	842
d	1.00	0.27	0.66	0.64	0.8
C		5	$5\ 10^5$	$5\ 10^{-4}$	10^7
x		1	-0.5	2	-1

Table 1: Set of parameters for each water category in MKS

2.2 Graupel growth modes

The graupels are very efficient collectors of cloud particles and hydrometeors because they sweep a large volume of air during their fall. Their surface temperature is generally warmer than the environmental temperature because the liquid accreted material releases latent heat. Until the mean surface temperature of the graupels T_g remains below 0° C, all the collected droplets and raindrops can freeze: this stage corresponds to the **DRY** growth mode. As soon as T_g reaches the melting point, a thin liquid film persists at the surface of the graupels and any excess of accreted liquid condensate is shed away: this second stage is the **WET** growth mode leading to the formation of hail embryos.

The graupel **DRY** growth scheme explicitly computes the individual collection rates of the cloud droplets, small ice crystals, raindrops and snowflakes. In the two last cases, look-up tables are necessary, otherwise integrations over the size distribution functions can be performed analytically. The **WET** growth is solution of the heat balance equation (Musil, 1970) with integration over the graupel spectrum and assuming $T_g = 0°$ C (shedding limit).

In the scheme, both **DRY** and **WET** rates are computed and compared, but only the lowest value is retained. For instance, **WET>DRY** means that enough water can freeze on the graupels so the growth can operate in the dry regime. Conversely if **DRY>WET**, the growth is in the wet mode because potentially accreting water cannot entirely freeze as **WET** represents the maximal freezing rate on the surface of the graupels.

2.3 Inclusion of a "hail" class of hydrometeor

The formation of hail particles is derived from the **WET** and **DRY** growth modes of the graupels. The partial conversion of graupels into hailstones is approximated by

$$\left.\frac{\partial r_h}{\partial t}\right|_{g\rightarrow h} = \left(\frac{\partial r_g}{\partial t}\right)^* \times \frac{\mathbf{DRY}}{\mathbf{DRY}+\mathbf{WET}}$$

where $(\partial r_g/\partial t)^*$ is the sum of the r_g tendences before the conversion into hail. The corresponding sink on the r_g budget is $\partial r_g/\partial t|_{g\rightarrow h} = -\partial r_h/\partial t|_{g\rightarrow h}$. The above formulation allows for a progressive transition from graupel to hailstone. It is based on the simple idea that the more the graupels can grow in the **WET** mode (**DRY≫WET** case), the more they are depleted and converted into hailstones. This macroscopic approach is in contrast with Ziegler (1985) who suggested a size distinction between graupel and hail which is based on a dry/wet growth threshold diameter to integrate by part over the graupel size distribution. We found that this technique is not easily applicable in a four class microphysical scheme insofar the scheme is rendered increasingly complex (Ferrier, 1994).

Once formed hail grows exclusively in the **WET** growth mode. No reverse conversion to the graupel category is possible for the moment. Hailstones fall and melt into rain at a rate, including ventilation effect, which is explicitly computed .

3. THE "MAP-IOP2a" CASE STUDY

3.1 Synpotic situation

Analysis for the 17 Sept. 1999 at 12UTC over Western Europe is taken from ECMWF (see Fig. 1). At the surface, a secondary low stands over Italy and induces a rapid flow (10 ms^{-1}) over the Adriatic Sea pointing to the northwestern italian Alps. At 500 hPa, an eastward moving trough over France advects cold and moist air over the LMTA and thus reinforces the development of deep convection in this area (the Milano-Linate soundings indicate a CAPE growth from 535 to 934 Jkg^{-1} between 12 and 18 UTC).

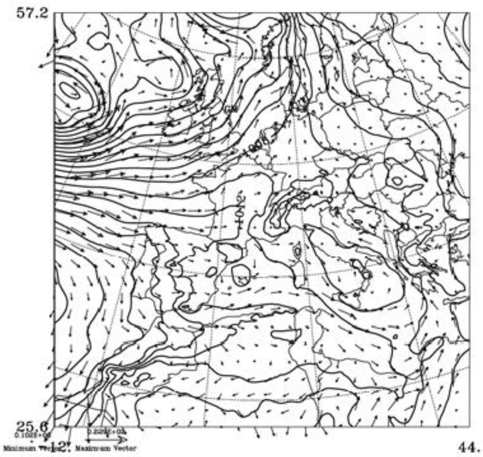

Figure 1: ECMWF surface chart of Sept. 17, 1999 at 12 UTC with SLP (contours every 2 hPa) and wind vectors.

3.2 Model set-up

The mesoscale model (MésoNH) is run with three levels of nesting on 50 uneven levels of altitude. The computational domains and topography are shown in Fig. 2. The 32 km mesh model (150× 150) follows the synpotic situation over Europe. The 8 km mesh domain (144 × 144) resolves the Alpine massif while the finest domain at 2 km resolution (160 × 160) is centered on the LMTA area. All the models start at 12 UTC and are integrated for 12 hours on a massively parallelized computer.

Four runs were performed to test the sensitivity to the microphysics but we restrict the result analysis for two of them. Run I3 uses the three-class (ice) standard scheme. Run I4 includes an explicit hail categorie. The simulated reflectivities Z (Ferrier, 1994) are filtered to ease the comparison with radar observations (Leise, 1981).

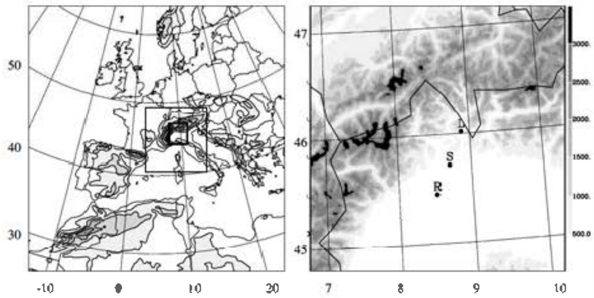

Figure 2: Geographical domains of the nested simulations (left) and the 2 km scale topography with 500 m contours on 160×160 grid points and R, S, L radar locations (right).

3.3 Results

Fig. **4** presents a hourly sequence of observed Z at $z = 2000$ m while the simulated Z for runs I3

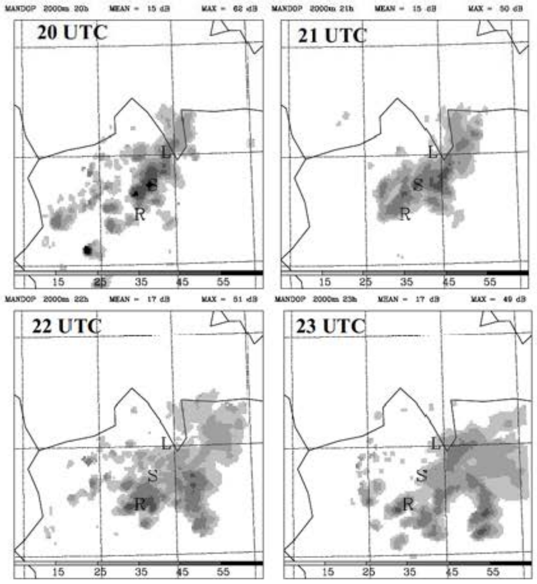

Figure 4: Observed Z at $z = 2000$ m

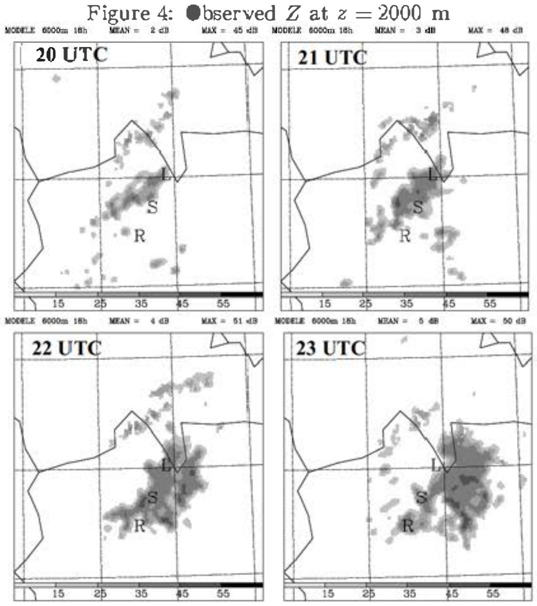

Figure 5: as in Fig. 4, but for Z from the I3 simulation

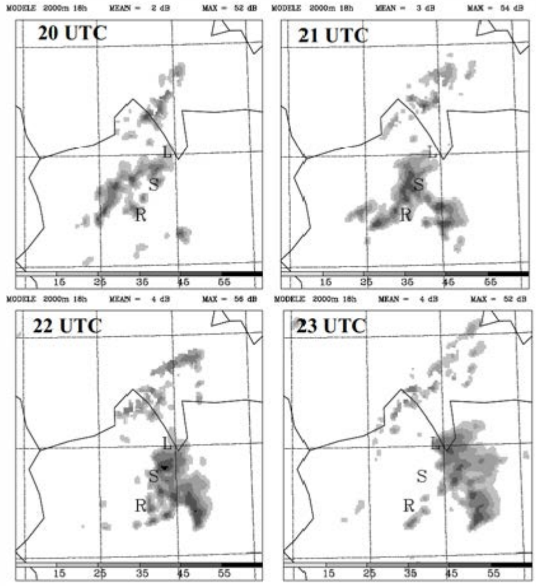

Figure 6: as in Fig. 4, but for Z from the I4 simulation

and I4 are given in Figs. 5 and 6, respectively. Although the observed radar echoes with $Z < 15$ dBZ ocupy a larger area, the location of the "horseshoe" pattern at 23 UTC is quite well reproduced in I3 and I4 simulations. Note also that Z is similar between I3 and I4 at 20 UTC after 8 hours of simulation but the southeast convective cluster seems to have a better positioning in I4 run. Looking now at at higher altitude ($z = 6000$ m in Figs 7-9), one can notice that only the I4 run is able to simulate the darkest spots ($Z > 55$ dBZ) which denote the presence of pure hail or graupel-hail mixture, as confirmed by the S-POL data analysis (Tabary et al., 2001). The "hot towers" are associated to intense updrafts ($w > 5$ ms^{-1}) as revealed by the Doppler radars.

To get a more precise view of the microphysical

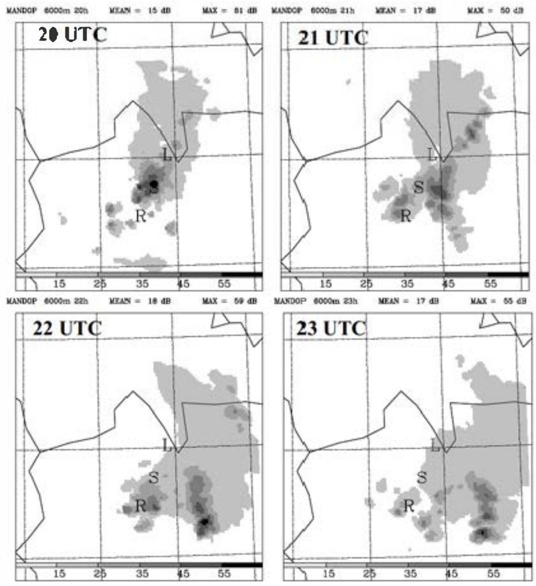

Figure 7: as in Fig. 4, but at $z = 6000$ m

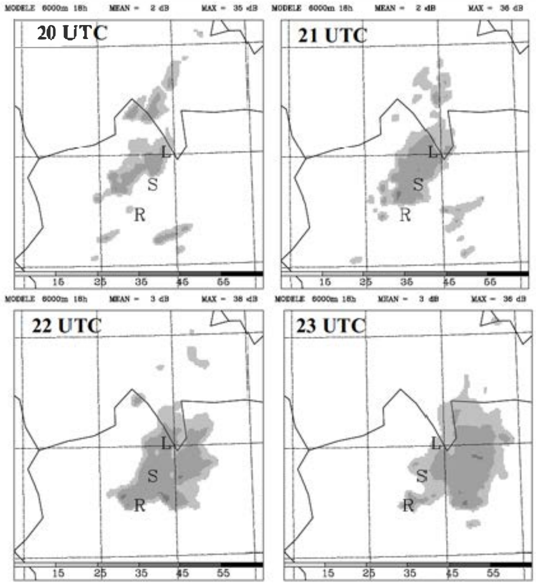

Figure 8: as in Fig. 5, but at $z = 6000$ m

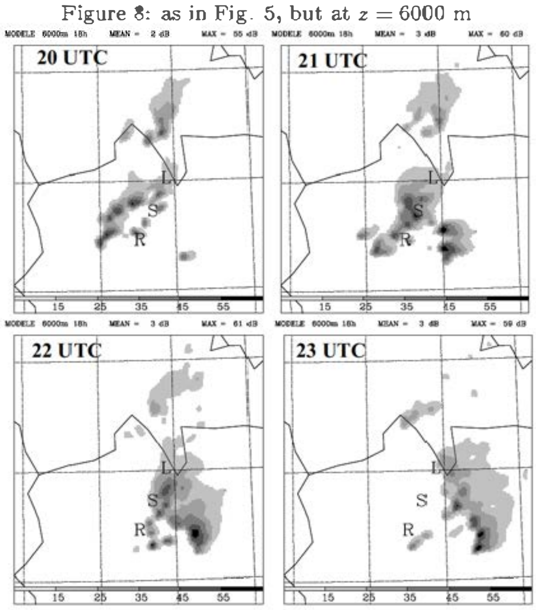

Figure 9: as in Fig. 6, but at $z = 6000$ m

characteristics of the convective cells in the southeast of the domain, two cross sections with S-POL particle classification and the corresponding simulation of particle amount, both valid at 22:30 UTC, are presented in Fig. 10. The S-POL radar data show that the turrets topping at 10-11 km contain a copious amount of hail "HL" (●) and hail-graupel mixture "GH" (**X**). This feature is quite well retrieved by run I4 of the model where the location of the hydrometeors with mixing ratios higher than 0.5 gkg^{-1} reveals a similar stratification of the microphysical composition of the precipitating system.

4. CONCLUSION

The ensemble of radar observations taken during MAP-IOP2a represents a unique database to study small-scale dynamical and microphysical interactions over orography. The explicit resolution of convection in a multiple nested mesoscale model provides encouraging results. Hail formation and location is reasonnably well captured by the four-class microphysical scheme compared to polarimetric data. Better results are expected in the future with model runs at 1 or 0.5 km scale resolution.

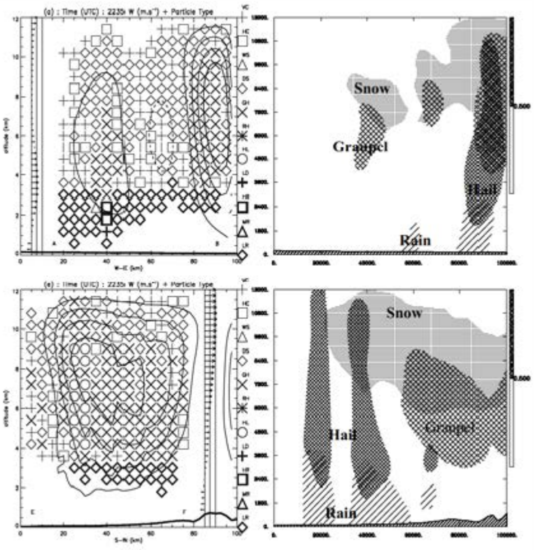

Figure 10: W-E (top) and S-N (bottom) vertical sections across the main convective cores at 22:30 UTC with S-POL particle classification and w (left) and modeled microphysics with threshold contour $r_r, r_s, r_g, r_h > 0.5$ gkg^{-1} (right).

5. REFERENCES

Bougeault, P., P. Binder, A. Buzzi, R. Dirks, R. Houze, J. Kuettner, R. B. Smith, R. Steinacker, H. Volkert and all the MAP scientists, 2001: The MAP special observing period. *Bull. Am. Meteor. Soc.*, **82**, 433-462.

Ferrier, B. S., W.-K. Tao, and J. Simpson, 1995: A double-moment multiple-phase four-class bulk ice scheme. Part II: Simulations of convective storms in different large-scale environments and comparisons with other bulk parameterizations. *J. Atmos. Sci.*, **52**, 1001-1033.

Lafore, J. P. and coauthors, 1998: The Meso-NH Atmospheric Simulation System. Part I: Adiabatic formulation and control simulations. *Annales Geophysicae*, **16**, 90-109.

Leise, J. A., 1981: A multidimensional scale-telescoped filter and data extension package. NOAA Tech. Memo. ERL WPL-82, 18 pp. [NTIS PB82-164104].

Musil, D. J., 1970: Computer modeling of hailstone growth in feeder clouds. *J. Atmos. Sci.*, **27**, 474-482.

Pinty, J.-P. and P. Jabouille, 1998: A mixed-phase cloud parameterization for use in a mesoscale non-hydrostatic model: simulations of a squall line and of orographic precipitation. In *Conf. on Cloud Physics*, Everett, WA. Amer. Meteor. Soc., 217-220.

Tabary, P., G. Scialom, and E. Richard, 2001: Four-dimensional structure of a mid-latitude orogenic squall line observed with Doppler/polarimetric radars during the MAP experiment. *Mon. Wea. Rev.*, in revision.

Ziegler, C. L., 1985: Retrieval of thermal and microphysical variables in observed concetive storms. Part I: Model development and preliminary testing. *J. Atmos. Sci.*, **42**, 1487-1509.